

Poloidal mode analysis of magnetic probe data in a spherical tokamak configuration^{a)}

H. Tojo,^{1,b)} A. Ejiri,¹ M. P. Gryaznevich,² Y. Takase,¹ and Y. Adachi¹

¹Graduate School of Frontier Sciences, The University of Tokyo, Kashiwa 277-8561, Japan

²EURATOM/UKAEA Fusion Association, Culham Science Centre, Oxfordshire OX14 3DB, United Kingdom

(Presented 14 May 2008; received 11 May 2008; accepted 7 July 2008;

published online 31 October 2008)

A method to determine the poloidal mode number m in a spherical tokamak based on magnetic probe data was developed. Perturbed magnetic fields at Mirnov coils are calculated for distributed helical filamentary currents on rational surfaces assuming the maximum current amplitude, m and n (toroidal mode number), and the toroidal location of the filaments. These free parameters were determined from the best fit to the measured signals. The residual error was reduced by a factor of 2 by introducing helical filaments instead of toroidal filaments. Using this method, $m/n=2/1$ and $3/2$ modes were identified in Mega-Ampere Spherical Tokamak discharges, and the time evolution of the tearing modes was derived. © 2008 American Institute of Physics.

[DOI: 10.1063/1.2965014]

I. INTRODUCTION

The determination of m is very important for the analysis of magnetohydrodynamic (MHD) instabilities, but in many tokamak experiments, it is not simple to determine m because of the noncircular shape of the plasma cross section. In spherical tokamak (ST), moreover, magnetic field configuration is different from conventional tokamak because of the strong inboard/outboard asymmetry in the magnetic field pitch angle. To overcome these problems we developed a method to identify the poloidal mode number and its intensity using a two-dimensional axisymmetric analysis.¹ However, there are two points we must improve. First, the previous methods did not use a continuous distribution of filamentary currents, which is necessary to represent continuous profiles of the plasma, such as temperature, pressure, and density. Second, three-dimensional effects should be taken into account. Since the area flattened by the tearing instability has a helical structure, we must calculate the effects of helical filaments to magnetic fields measured by Mirnov coils from more than one poloidal cross section. These effects are not negligible in ST configurations with low aspect ratio. The goal of this work is to determine the m from the experimentally measured signals of Mirnov coils (magnetic probes) with minimum error. Reducing error is very important for the determination of m in low signal to noise ratio condition, and it is also effective for identifying inferior modes, which may show a nonlinear rapid growth just before MHD instabilities. We performed these analyses including the effects mentioned above in the Mega-Ampere Spherical Tokamak (MAST).² In MAST, Mirnov coils are located along the center column (up to 40 channels) and along the

outboard side (up to 18 channels) on a poloidal cross section. Figure 1 (black points) shows the positions of Mirnov coils. All of these coils measure the vertical magnetic field (B_z). It is necessary to determine the trajectories of filamentary currents on rational surfaces in order to represent the mode structure. Tearing modes are localized on rational surfaces such as $q=1, 1.5, 2, 3$, where q is the safety factor. We calculated trajectories of magnetic field lines on each rational surface based on equilibrium fitting (EFIT) reconstruction³ on MAST with aspect ratio $A < 1.5$. Once vertical (B_z), radial (B_R), and toroidal (B_t) magnetic fields are obtained, the tangents (trajectories) of the field lines is given by $d\phi/d\theta = (r/R)[B_t/(-B_R \sin \theta + B_z \cos \theta)]$, where ϕ , θ , r , and R are the toroidal angle, the poloidal angle, distance from the magnetic axis to a point on the rational surface, and the distance from the symmetry axis of the torus to the point. Figure 2 shows field line trajectories in a typical discharge. Zero on the poloidal turn corresponds to the $z=0$ plane on the outboard side. The slope is steep on the inboard side because the ratio of the toroidal magnetic field to the poloidal magnetic field is stronger. This is a characteristic of STs.

II. AXISYMMETRIC AND HELICAL CONFIGURATION WITH DISTRIBUTED FILAMENTARY CURRENTS

For a high aspect ratio circular cross section plasma, distributed filamentary currents with a given mode structure can be written as $I_{mni}(\theta, \phi) = I_0 \exp i[m\theta - n(\phi + \phi_l + \phi_0)]$. I_0 , ϕ_l , and ϕ_0 are maximum filamentary current, equally spaced toroidal angle with respect to the number of distributed filaments (if the number is 4, $\phi_l=0, \pi/2, \pi, 3\pi/2$), and toroidal angle (offset) as initial condition, respectively. However, this formula is not valid for a low aspect ratio or a noncircular cross section plasma. In general toroidal plasmas we can represent ϕ as a function of θ as shown in Fig. 1. Therefore we can describe helical filamentary currents as $I_{mni}(\theta, \phi) = I_0 \exp in[\phi(\theta) - \phi + \phi_l + \phi_0]$. This formula indicates that the

^{a)} Contributed paper, published as part of the Proceedings of the 17th Topical Conference on High-Temperature Plasma Diagnostics, Albuquerque, New Mexico, May 2008.

^{b)} Electronic mail: tojo@fusion.k.u-tokyo.ac.jp.

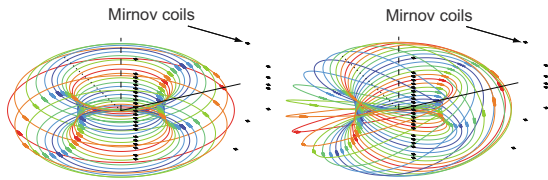


FIG. 1. (Color online) Models with axisymmetric (left) and helical (right) filaments.

distribution of filamentary currents at a poloidal cross section is decided by trajectories of Fig. 2. When we decide one initial toroidal position (ϕ_0), poloidal angles of other filaments are chosen by toroidal intervals. The distance of the intervals depends on m and the number of distributed points (ϕ_l). There are two ways to represent a filamentary structure. One is by axisymmetric filaments (parallel to the toroidal direction), which is almost the same as that in Ref. 1. The other is by the helical filaments (parallel to the magnetic field lines). Since islands induced by tearing modes have a helical structure, trajectories of the currents should have the same structure. Figure 1 shows examples of distributed filamentary currents with a $3/2$ mode at $q=1.5$ in both filament configurations. Generally, one peak of the filamentary currents appears outboard side and this is consistent with the small tangent (Fig. 2 at $q=1.5$) caused by a weak toroidal magnetic field.

III. COMPARISON WITH EXPERIMENTAL RESULTS

The helical filaments require heavier computational resources than the axisymmetric filamentary configuration. Thus, it is important to evaluate this helical effect qualitatively, and see how large the effect is. We calculated magnetic fields on a (virtual) surface with minor radius of $r_m=0.8$ m using a MAST configuration. Figure 3 shows the poloidal (B_p) and toroidal (B_t) magnetic fields for the $m/n=3/2$ mode as a function of the poloidal angle. Fifteen filaments are used to generate the magnetic fields. The major difference between these calculations is the existence of finite B_t for the helical filaments, which is absent for the axisymmetric filaments. It is generated by the helical effect, i.e., by the vertical components of the currents. Crosses describe poloidal angle of the filaments with the maximum or the minimum current. The dotted lines indicate amplitude ad-

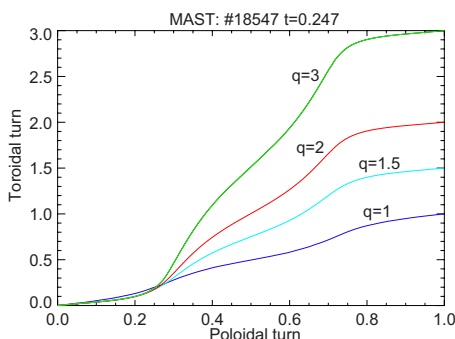


FIG. 2. (Color online) Trajectories of magnetic field lines on different rational surfaces from EFIT reconstruction (# 18547, $t=0.247$ s). Although the minimum q is larger than 1 in this configuration, the trajectory on the $q=1$ surface is created artificially to represent a possible $m=1$ mode.

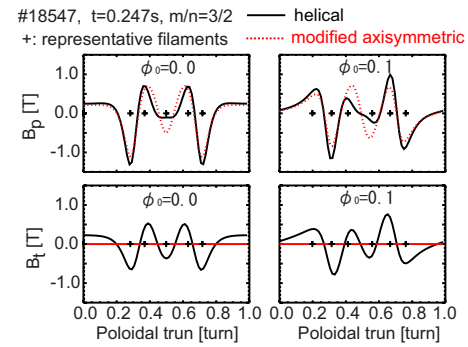


FIG. 3. (Color online) Poloidal (upper) and toroidal (bottom) magnetic fields calculated for helical and axisymmetric filamentary configurations at $r_m=0.8$ m using 72 poloidal points.

justed axisymmetric results such that the discrepancy with the helical calculation is minimized in a least-squares sense. Note that these adjusted results are obtained by a least-squares method. Even if the amplitude is adjusted, the discrepancy between these two configurations is significant. Especially, in the high-field side, the difference is not negligible because the pitch angle is small and the toroidal variation of the current is larger than the situation in the low-field side. The close filaments with alternating currents can easily offset the field at the measurement points. We performed these calculations for the MHD mode observed by the Mirnov coils. In a discharge, magnetic fluctuations with a few kilohertz are observed before an MHD event ($t\sim 0.25$ s in Fig. 4), which causes collapse of plasma and is called IRE.¹ The mode in-

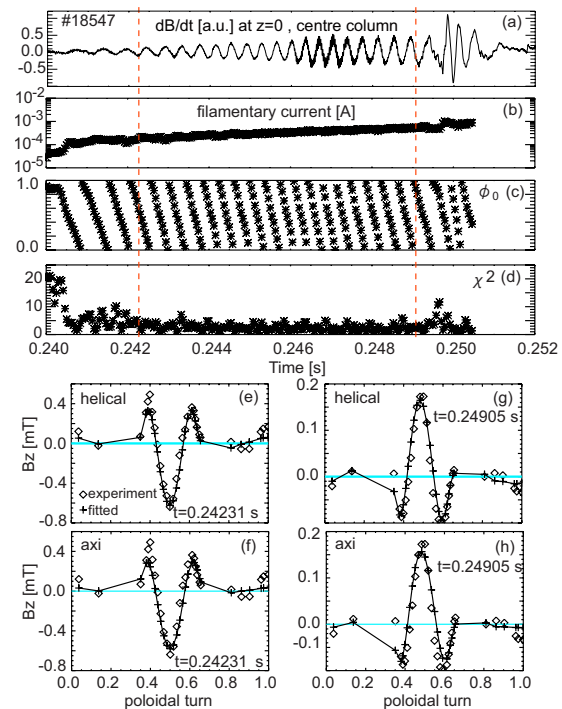


FIG. 4. (Color online) Time evolution of the fitted result using helical filaments. ($m/n=2/1$ mode) (a) Mirnov coil signal at $z=0$, dB/dt (a.u.). (b) The maximum current of filamentary currents (A). (c) The toroidal angle offset (turns). (d) χ^2 (fitting error). Bottom figures show the vertical magnetic fields (B_z) measured by Mirnov coils and fitted results using helical and axisymmetric filaments at $t=0.24231$ s [(e) and (f)] and 0.24950 s [(g) and (h)], indicated by red lines in the top figure.

tensity and the mode number were determined from the two parameters: one is the maximum current in the distributed filaments and the other is the toroidal angle (offset, ϕ_0) for the initial filament. The toroidal angle determines the filament positions uniquely, and its time evolution represents the toroidal rotation of the mode. The results are shown in Fig. 4. Before applying the method, we used a band-passed filter (1–5 kHz) and performed time integration to obtain filtered magnetic fields. Most cases show good agreement between the measured and calculated data assuming only $m/n=2/1$ mode.

To evaluate goodness of the fit, the residual error χ^2 was calculated. rms fluctuation amplitude was employed for the variance. When χ^2 is less than 10, the phase relations and amplitudes of these calculated and measured results look acceptable in the present analysis. The mode intensity is given by the fitted filamentary currents [Fig. 4(b)] and shows linear growth with a time constant of about 2 ms. The monotonic increase of the toroidal offset (ϕ_0) in Fig. 4(c) represents a toroidal rotation of filamentary currents. The accuracy of the fit is acceptable from $t=0.2405$ to 0.2505 s as shown in Fig. 4(d). Fittings with helical and axisymmetric filaments were performed and compared. It indicates superiority of the helical filaments. For instance, at $t=0.24231$ s, χ^2 are 1.91 (helical) and 3.78 (axisymmetric), and at $t=0.249050$ s, 2.16 (helical) and 5.84 (axisymmetric). In some cases, however, the residual error for axisymmetric filaments becomes very large. Therefore, helical filaments are used hereafter.

In a case of $m/n=3/2$ mode, reasonable fitting results have also been obtained. The power spectra of the Mirnov coil data show a mode with high (~ 20 kHz) frequency. Unfortunately, the residual error χ^2 is not as small as shown in Fig. 5. The values are roughly more than 10. The reasons for such high errors compared with the $2/1$ mode are as follows.

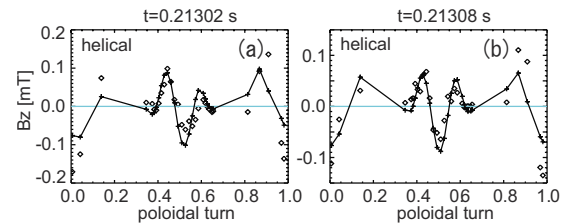


FIG. 5. (Color online) Comparison between the vertical magnetic fields (B_z) measured by Mirnov coils and fitted results using helical filaments at $t=0.21302$ s (a) and 0.21308 s (b).

(1) EFIT without internal measurement has some error in positions of rational surfaces when the surface is located in the low shear region. (2) Intensity of Mirnov coil signals for the $3/2$ mode is smaller than for the $2/1$ mode because the $3/2$ mode is localized at $q=1.5$, which is far from the Mirnov coils. Figure 5 shows the fitting results at two different times. The signals with 18–25 kHz components are used for fitting. The toroidal offset (ϕ_0) indicates toroidal rotation of the mode.

ACKNOWLEDGMENTS

This work was supported by JSPF Grant-in-Aid for Scientific Research 16106013 and NIFS/NINS under the project of Formation of International Network for Scientific Collaborations.

¹H. Tojo, M. P. Gryaznevich, A. Ejiri, A. Sykes, and Y. Takase, *Plasma Fusion Res.* **3**, S1065 (2008).

²B. Lloyd, J.-W. Ahn, R. J. Akers, L. C. Appel, E. R. Arends, K. B. Axon, R. J. Buttery, C. Byrom, P. G. Carolan, C. Challis *et al.*, *Nucl. Fusion* **43**, 1665 (2003).

³L. Lao, H. St. John, R. D. Stambaugh, A. G. Kellman, and W. Pfeiffer, *Nucl. Fusion* **25**, 1611 (1985).